

ARTICLE



Chemokine receptor CCR9 suppresses the differentiation of CD4⁺CD8α⁺ intraepithelial T cells in the gut

Can Li¹, Hye Kyung Kim², Praveen Prakhar¹, Shunqun Luo¹, Assiatu Crossman¹, Davinna L. Ligons¹, Megan A. Luckey¹, Parirokh Awasthi³, Ronald E. Gress² and Jung-Hyun Park¹✉

This is a U.S. Government work and not under copyright protection in the US; foreign copyright protection may apply 2022

The chemokine receptor CCR9 equips T cells with the ability to respond to CCL25, a chemokine that is highly expressed in the thymus and the small intestine (SI). Notably, CCR9 is mostly expressed on CD8 but not on CD4 lineage T cells, thus imposing distinct tissue tropism on CD4 and CD8 T cells. The molecular basis and the consequences for such a dichotomy, however, have not been fully examined and explained. Here, we demonstrate that the forced expression of CCR9 interferes with the tissue trafficking and differentiation of CD4 T cells in SI intraepithelial tissues. While CCR9 overexpression did not alter CD4 T cell generation in the thymus, the forced expression of CCR9 was detrimental for the proper tissue distribution of CD4 T cells in the periphery, and strikingly also for their terminal differentiation in the gut epithelium. Specifically, the differentiation of SI epithelial CD4 T cells into immunoregulatory CD4⁺CD8α⁺ T cells was impaired by overexpression of CCR9 and conversely increased by the genetic deletion of CCR9. Collectively, our results reveal a previously unappreciated role for CCR9 in the tissue homeostasis and effector function of CD4 T cells in the gut.

Mucosal Immunology (2022) 15:882–895; <https://doi.org/10.1038/s41385-022-00540-9>

INTRODUCTION

T cell development in the thymus is driven by a series of precisely timed and spatially controlled signaling events. Guiding the developing thymocytes through the thymus in coordination with these signals is mediated by a combination of chemotactic cues that utilize chemokine receptors, such as CXCR4, CCR7, and CCR9¹. CXCR4 binds the chemokine SDF-1, which is highly expressed in the thymic cortex and prevents the premature entrance of immature thymocytes into the medulla^{2,3}. CCR7, on the other hand, responds to the chemokines CCL19 and CCL21 which are abundant in the thymic medulla and which attract post-selection thymocytes for their further maturation and differentiation⁴. A role for CCR9 in the intrathymic trafficking of thymocytes, however, remains unclear. The CCR9 ligand, CCL25, is highly expressed by cortical thymocytes⁵, so that CCR9 could potentially contribute to the recruitment of immature thymocytes into the cortex. However, pre-selection thymocytes are refractory to CCR9 signaling⁶, and CCR9-deficient (*Ccr9*^{-/-}) mice do not display discernible defects in thymic T cell differentiation^{7,8}, suggesting that CCR9 would not play a major role in this process. Nonetheless, CCR9 remains of particular interest because its expression is not only associated with T cell maturation but also with CD4 versus CD8 T cell lineage differentiation. As such, CCR9 is abundantly expressed on immature CD4⁺CD8⁺ double-positive (DP) thymocytes but selectively downregulated upon CD4 lineage commitment, so that CD8 T cells maintain—but CD4 T cells lack—expression of CCR9⁹. Such a dichotomy is unique to CCR9, because CCR7 is

highly expressed on both CD4 and CD8 T cells while CXCR4 is absent on both CD4 and CD8 T cells. Thus, CCR9 is a lineage-associated chemokine receptor whose selective expression on CD8 T cells is established during T cell development in the thymus.

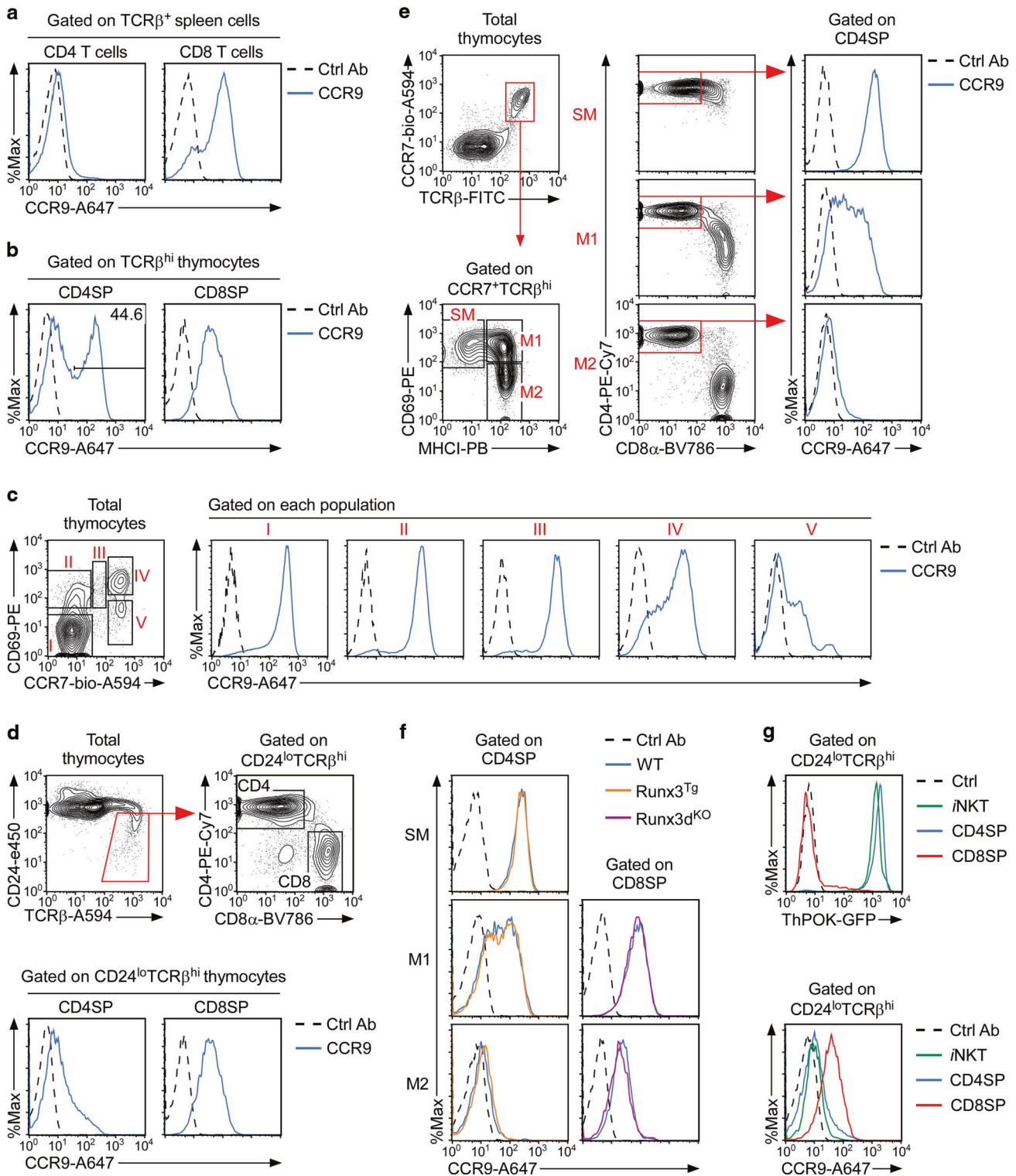
Our understanding of the transcriptional and/or epigenetic mechanisms that impose such CD8 T cell-specific expression of CCR9 is still in its infancy^{10,11}. In this regard, it remains uncertain what signals would selectively downregulate CCR9 expression on CD4 T cells or what factors would drive CCR9 expression on CD8 T cells. On the other hand, the requirement for CCR9 on T cells has been assessed in many venues, including the analyses of *Ccr9*^{-/-} mice, where CCR9-deficiency was found to impair the recruitment of CD8 T cells into small intestine (SI) intraepithelial tissues and to hamper the establishment of oral immune tolerance^{7,12}. Thus, CCR9 provides critical cues for the recruitment and tissue-specific function of CD8 T cells. In fact, a physiological role for CCR9 has been evident for the tissue tropism of peripheral CD8 T cells where CCR9 was found to facilitate the colonization of SI intraepithelial T cells⁷. CCL25 is highly expressed in intestinal tissues, and CCR9 expressed on CD8 T cells equips them with CCL25 sensitivity, thus promoting their recruitment to the gut¹³.

Importantly, while most CD4 T cells lack CCR9 expression, CCR9 is not completely absent on all CD4 T cells. In fact, a subset of gut homing Foxp3⁺ Treg cells and a fraction of CD4⁺ T cells among intraepithelial lymphocytes (IELs) in the SI show clear expression of CCR9¹⁴. The CCR9 expression on CD4 IEL T cells is thought to be induced by their interaction with CD103⁺ dendritic cells in the gut

¹Experimental Immunology Branch, Center for Cancer Research, National Cancer Institute, NIH, Bethesda, MD 20892, USA. ²Experimental Transplantation and Immunotherapy Branch, Center for Cancer Research, National Cancer Institute, NIH, Bethesda, MD 20892, USA. ³Laboratory Animal Sciences Program, Leidos Biomedical Research Inc., Frederick National Laboratory for Cancer Research, National Institute of Health, Frederick, MD 21701, USA. ✉email: parkhy@mail.nih.gov

Received: 10 December 2021 Revised: 5 June 2022 Accepted: 8 June 2022

Published online: 1 July 2022



which produce the vitamin A metabolite retinoic acid (RA), a transcriptional regulator of CCR9¹¹. Therefore, environmental cues in the gut epithelium can induce CCR9 expression on CD4 T cells once they migrate into the intestinal tissues. CD4 IEL T cells are derived from conventional CD4 T cells, and they are commonly referred to as induced IELs (iIELs). The iIELs differ from natural IELs (nIELs) which are generated by agonistic selection in the thymus and undergo post-thymic differentiation in the intestine. nIELs are mostly comprised of CD8 T cells, and they are marked by

expressing CD8 $\alpha\alpha$ homodimers, instead of conventional CD8 $\alpha\beta$ heterodimers, as coreceptors¹⁵. The exact role of CD8 $\alpha\alpha$ nIELs versus CD8 $\alpha\beta$ iIELs in gut immunity is not fully understood^{16–18}. However, the expression of CD8 $\alpha\alpha$ homodimers is highly induced by the gut environment, and it is well established that CD4 iIELs also can acquire such traits of CD8 $\alpha\alpha$ expression through transcriptional reprogramming¹⁹, so that the differentiation of CD4 iIELs into CD4 $^+$ CD8 $\alpha\alpha$ $^+$ DP IEL T cells is accompanied by the acquisition of cytotoxic effector function²⁰. Consequently,

Fig. 1 CCR9 downregulation is associated with CD4 lineage specification. **a** CCR9 expression was assessed on CD4 and CD8 spleen T cells. Results are representative of 14 independent experiments with a total of 16 WT mice. **b** CCR9 expression was assessed on TCR β^{hi} mature CD4SP and CD8SP thymocytes. Results are representative of 14 independent experiments with a total of 16 WT mice. **c** Total thymocytes were assessed for CCR7 and CD69, whose differential expression identifies 5 distinct developmental stages of thymocytes (i.e., stages I–V). CCR9 expression was then assessed for each stage. Results are representative of 6 independent experiments with a total of 8 WT mice. **d** CCR9 expression on CD24 $^{\text{lo}}$ TCR β^{hi} mature CD4SP and CD8SP thymocytes. Results are representative of 6 independent experiments with a total of 6 WT mice. **e** CCR9 expression on post-selection CD4SP thymocytes. Post-selection (CCR7 $^{+}$ TCR β^{hi}) thymocytes were identified by CCR7 and TCR β expression and then assessed for further maturation based on CD69 and MHCI expression (left). CCR9 expression was determined in CD4SP cells from semi-mature (SM), mature 1 (M1) or mature 2 (M2) thymocyte populations (right). The results are representative of 5 independent experiments with a total of 9 WT mice. **f** CCR9 expression on Runx3 $^{\text{Tg}}$ and Runx3d $^{\text{KO}}$ thymocytes. CCR9 expression was determined on post-selection CD4SP cells of SM, M1, and M2 thymocytes of WT and Runx3 $^{\text{Tg}}$ mice (left), and on post-selection CD8SP cells of M1 and M2 thymocytes of WT and Runx3d $^{\text{KO}}$ mice (right). Results are representative of 3 independent experiments with a total of 5 WT, 6 Runx3 $^{\text{Tg}}$, and 4 Runx3d $^{\text{KO}}$ mice. **g** ThPOK-GFP reporter (top) and CCR9 expression (bottom) on CD24 $^{\text{lo}}$ TCR β^{hi} mature CD4SP, CD8SP, and *i*NKT cells of ThPOK-GFP reporter thymocytes. Results are representative of 2 independent experiments with a total of 3 ThPOK-GFP reporter mice.

CD4 $^{+}$ CD8 $\alpha\alpha^{+}$ DP IELs correspond to MHCII-restricted cytolytic T cells and they may play critical niche functions in intestinal immunity²⁰. Because both CD4 iIELs and DP IELs are derived from conventional CD4 T cells, we wished to understand the impact of CCR9 on the gut tropism of CD4 T cells and the differentiation of DP IELs.

To this end, here, we established a genetically engineered mouse model where CCR9 is forced to be expressed on CD4 T cells. In such CCR9-transgenic (CCR9 $^{\text{Tg}}$) mice, we found that CD4 T cell development in the thymus was unaffected, but that the tissue tropism of peripheral CD4 T cells was substantially altered. We observed a significant loss in splenic CD4 T cells concomitant to an increased accumulation of CD4 T cells in mesenteric lymph nodes (mLNs). Also, contrary to our expectation, the forced expression of CCR9 on CD4 T cells did not promote but was detrimental for populating the CD4 iIEL pool. Most strikingly, the frequency and number of DP IELs were dramatically decreased in CCR9 $^{\text{Tg}}$ mice, thus revealing a new regulatory pathway of CD4 T cell trafficking where CCR9 plays a detrimental role in establishing CD4 IEL immunity.

RESULTS

CCR9 downregulation is associated with CD4 lineage differentiation

CCR9 is selectively expressed on CD8 lineage T cells so that CCR9 is abundant on CD8 but conspicuously absent from CD4 T cells (Fig. 1a)⁹. To understand why CD4 T cells downregulate CCR9 expression, we first aimed to understand what determines the lineage-specific expression of CCR9. To this end, we assessed CCR9 expression on mature CD4 and CD8 single-positive (SP) cells in the thymus, the site of their generation. CCR9 was abundantly expressed on all CD8SP thymocytes, and interestingly also on a substantial fraction of thymic CD4 T cells (Fig. 1b). Thus, unlike peripheral CD4 T cells (Fig. 1a), newly generated CD4SP thymocytes do express CCR9, and such thymic CD4 T cells presumably require further maturation to fully downregulate CCR9.

To further assess the developmental dynamics of CCR9 expression, we employed the combined staining for CD69 and CCR7 which visualizes 5 distinct stages in T cell development (Fig. 1c)³. Stage I and II correspond to pre-selection thymocytes and stage IV and V correspond to post-selection thymocytes³. Thymocytes that appear as CD69 $^{+}$ CCR7 $^{\text{int}}$ (stage III) are undergoing positive selection (Fig. 1c)³. CCR9 was highly expressed on all immature thymocytes (stages I–III), but downregulated in post-selection thymocytes (stage IV and V) (Fig. 1c). Moreover, the amount of surface CCR9 further decreased with maturation, so that CCR9 abundance was considerably diminished in late stage thymocytes (stage V) compared to less mature stage IV thymocytes (Fig. 1c and Supplementary Fig. 1a). In fact, the most mature CD4SP thymocytes which are found in the CD24 $^{\text{lo}}$ TCR β^{hi}

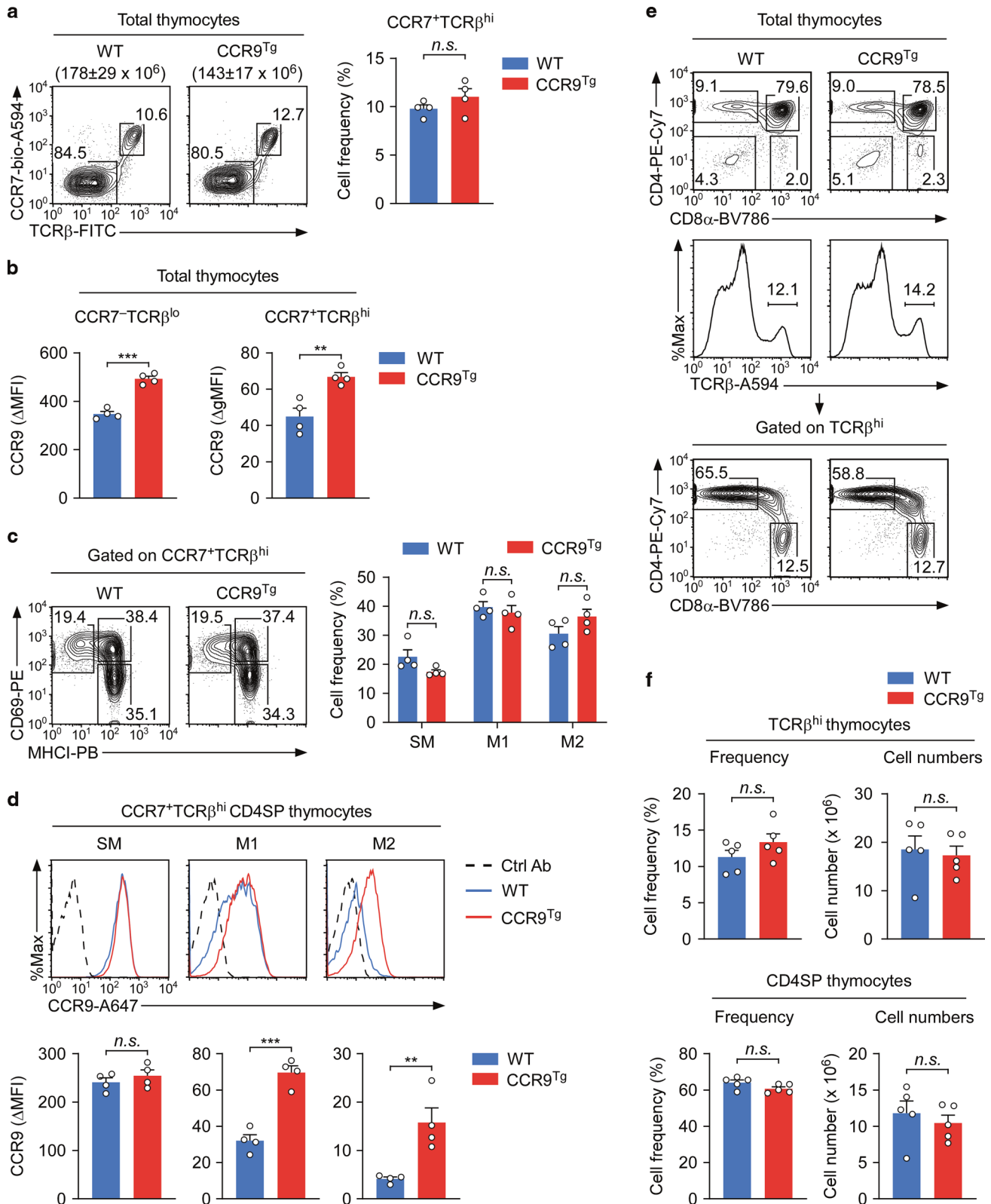
population, showed substantial loss of CCR9 (Fig. 1d). Collectively, these results indicated that CCR9 downregulation is a cellular process that is tightly associated with the lineage specification and maturation of CD4 T cells.

Forced expression of Runx3 fails to prevent CCR9 downregulation in CD4 T cells

Having established that CCR9 downregulation is initiated upon CD4 lineage commitment and that further maturation is required to extinguish CCR9 expression on CD4 T cells, we next aimed to monitor this process in detail. To this end, we gated on post-selection thymocytes (CCR7 $^{+}$ TCR β^{hi})²¹, and assessed their CCR9 expression as they underwent further thymic maturation. Positively selected thymocytes can be divided into three distinct developmental stages based on CD69 and MHCI expression²¹. CD69 $^{+}$ MHCI $^{-}$ cells are developmentally semi-mature (SM), which proceed to mature stage 1 (M1; CD69 $^{+}$ MHCI $^{+}$) before achieving full maturation as mature stage 2 cells (M2; CD69 $^{+}$ MHCI $^{+}$) (Fig. 1e, left). Notably, CCR9 expression on CD4SP cells showed a gradual downregulation from SM over M1 into M2 (Fig. 1e, right). Thus, the loss of CCR9 is a developmentally controlled process that is linked with post-selection maturation and completed in fully mature CD4SP thymocytes.

To gain further insight into the molecular basis of CCR9 downregulation, we next asked whether the transcriptional pathways that determine CD4 versus CD8 lineage fate would be involved in this process. The Runt-related transcription factor Runx3 specifies CD8 T cell fate. In agreement, the distal promoter-driven Runx3 (Runx3d) is highly induced upon CD8 lineage commitment but absent in CD4 T cells²². Such distinct Runx3 expression correlates with CCR9 expression in post-selection thymocytes, suggesting a potential association of Runx3 and CCR9 expression in mature T cells. To examine if Runx3 is required to drive CCR9 expression on CD8 T cells, and, conversely, whether Runx3 would be sufficient to induce CCR9 expression on CD4 T cells, we examined CCR9 expression in Runx3d-deficient (Runx3d $^{\text{KO}}$)²³ and Runx3-transgenic (Runx3 $^{\text{Tg}}$) mice²⁴. In Runx3d $^{\text{KO}}$ mice (Supplementary Fig. 1b), we found that CCR9 was still abundantly expressed on CD8SP thymocytes and spleen CD8 T cells (Fig. 1f, right and Supplementary Fig. 1c, d), suggesting that Runx3 is not required for CCR9 expression on CD8 T cells. On the other hand, CD4SP thymocytes and CD4 T cells that are forced to express Runx3 still failed to induce CCR9 (Fig. 1f, left and Supplementary Fig. 2)²⁴, indicating that CD4 lineage-specific downregulation of CCR9 is not because of lacking Runx3.

While Runx3 specifies CD8 lineage commitment, the zinc finger transcription factor ThPOK specifies CD4 lineage differentiation^{25,26}. As such, if CCR9 downregulation would be associated with CD4 lineage commitment, we would predict that CCR9 downregulation would correlate with ThPOK expression. Interestingly, the protein abundance of ThPOK was significantly reduced in SI IEL CD4 T cells compared to spleen CD4 T cells, and CCR9



expression was conversely increased upon diminished ThPOK expression in SI IEL CD4 T cells (Supplementary Fig. 3a). Such an inverse relationship between ThPOK and CCR9 expression was further documented by using ThPOK-GFP gene reporter mice²⁷, where we found ThPOK transcription being conversely correlated with the loss of CCR9 expression in mature T cells (Fig. 1g).

Invariant natural killer T (iNKT) cells represent another major T cell population in the thymus that expresses ThPOK (Fig. 1g, top)^{28,29}. Unlike CD4 T cells, however, iNKT cells are selected by MHCII-like CD1d molecules and they are not MHCII-restricted as is the case for conventional CD4 T cells²⁹. If ThPOK would be a negative regulator of CCR9, iNKT cells should have terminated

Fig. 2 Forced CCR9 expression does not interfere with CD4SP thymocyte development. **a** Identification of pre- (CCR7⁺TCRβ^{lo}) and post-selection (CCR7⁺TCRβ^{hi}) thymocytes of WT and CCR9^{Tg} mice. Total thymocyte numbers are listed on the top. Bar graph shows post-selection thymocyte frequencies as a summary of 4 independent experiments with a total of 4 WT and 4 CCR9^{Tg} mice. **b** Graphs show the delta Median Fluorescence Intensity (ΔMFI) and geometric Mean Fluorescence Intensity (ΔgMFI) of CCR9 on pre- and post-selection thymocytes of WT and CCR9^{Tg} mice, respectively. Data are from 4 independent experiments with a total of 4 WT and 4 CCR9^{Tg} mice. **c** Contour plots show the SM, M1, and M2 distribution of post-selection thymocytes in WT and CCR9^{Tg} mice. Data are from 4 independent experiments with a total of 4 WT and 4 CCR9^{Tg} mice. Statistical significance was determined by two-way ANOVA with Sidak's multiple comparisons test. **d** Surface abundance of CCR9 was determined on SM, M1, or M2 CD4SP thymocytes of WT and CCR9^{Tg} mice. Histograms (top) are representative and bar graphs (bottom) show summary from 4 independent experiments with a total of 4 WT and 4 CCR9^{Tg} mice. **e** CD4 versus CD8 profiles of total (top) and TCRβ^{hi}-gated (middle) mature thymocytes (bottom) of WT and CCR9^{Tg} mice. Data are representative of 5 independent experiments with a total of 5 WT and 5 CCR9^{Tg} mice. **f** Frequencies and numbers of TCRβ^{hi} (top) and mature CD4SP thymocytes (bottom) from WT and CCR9^{Tg} mice. Data show summary of 5 independent experiments with a total of 5 WT and 5 CCR9^{Tg} mice. Data are shown as mean ± SEM. ****P* < 0.01, ***P* < 0.001, *n.s.*, not significant.

CCR9 expression because they express ThPOK. Indeed, *i*NKT cells expressed large amounts of ThPOK-GFP reporter protein but little CCR9 (Fig. 1g, bottom). To directly demonstrate ThPOK-induced suppression of CCR9, we next employed ThPOK-transgenic (ThPOK^{Tg}) mice (Supplementary Fig. 3b)³⁰, and examined CCR9 expression on SI IEL CD4 T cells. Here, we found that ThPOK overexpression effectively downregulated CCR9 expression on ThPOK^{Tg} SI IEL CD4 T cells (Supplementary Fig. 3c), proposing a direct inhibitory role for ThPOK on CCR9 expression. Altogether, these results indicate that ThPOK expression correlates with CCR9 downregulation, which could be explained by a ThPOK-driven regulatory circuitry of CCR9 regulation in mature T cells. But, this remains to be experimentally tested.

Forced CCR9 expression on CD4SP thymocytes

Because CCR9 downregulation parallels the maturation of CD4 T cells, we next wanted to know whether CCR9 downregulation was required for CD4 T cell development in the thymus. To this end, we generated CCR9 transgenic mice (CCR9^{Tg}) that overexpress the murine *Ccr9* cDNA under the control of human *CD2* regulatory elements so that CCR9 is constitutively overexpressed on all T lineage cells. We confirmed the successful transgene expression in two independent founder lines (Supplementary Fig. 4), and we utilized the transgene which expressed greater amounts of CCR9, i.e. the L4 line, for the rest of this study.

Pre-selection and post-selection thymocytes can be identified by their distinct expression of CCR7 and TCRβ (Fig. 2a)²¹. While CCR7⁺TCRβ^{lo} pre-selection thymocytes of CCR9^{Tg} mice expressed large amounts of CCR9 (Fig. 2a, b), we also found significantly increased levels of CCR9 on CCR7⁺TCRβ^{hi} post-selection thymocytes (Fig. 2b), indicating that CCR9 is overexpressed throughout the T cell development of CCR9^{Tg} mice. Notably, the total thymocyte numbers (Fig. 2a), and the frequency of CCR7⁺TCRβ^{hi} mature thymocytes did not significantly differ between CCR9^{Tg} and WT littermate controls (Fig. 2a). These results show that the CCR9 overexpression did not interfere with T cell development in the thymus. To specifically assess CCR9 expression during CD4SP cell maturation, we next examined the CCR9 abundance on SM, M1, and M2 CD4SP thymocytes of WT and CCR9^{Tg} mice (Fig. 2c and Supplementary Fig. 5). CCR9 expression was significantly increased in M1 and M2 thymocytes of CCR9^{Tg} mice (Fig. 2d), but CCR9 overexpression did not alter the frequency and number of CD4SP cells (Fig. 2e, f), which compares to the minimal perturbation of CD4SP cell generation in CCR9-deficient mice^{7,8}. Collectively, these data indicated that the forced expression of CCR9 did not disturb the thymic generation of CD4SP cells.

CCR9^{Tg} CD4 T cells accumulate in mesenteric lymph nodes

To explore whether the forced expression of CCR9 would affect CD4 T cells in peripheral tissues, we next examined splenic T cells in WT and CCR9^{Tg} mice. In CCR9^{Tg} mice, CCR9 was overexpressed on all CD8 T cells (Supplementary Fig. 6) and ectopically expressed

on CD4 T cells (Fig. 3a, top). The abundance of other chemokine receptors, such as CCR7, however, remained unaltered (Fig. 3a, bottom).

CCR9 mediates the chemotaxis to CCL25, the only known ligand for this chemokine receptor³¹. To examine whether the forced expression of CCR9 had functional consequences, we performed transwell migration assays for CCL25 using naive CD4 T cells from WT or CCR9^{Tg} mice. As shown in Fig. 3b, CCR9^{Tg} CD4 T cells showed substantially increased CCL25 responsiveness, demonstrating that the forced expression of CCR9 equips CD4 T cells with the ability to respond to CCL25. Possibly due to such acquired CCL25 sensitivity, CCR9^{Tg} CD4 T cells were mobilized, resulting in significantly reduced cell numbers in the spleen of CCR9^{Tg} mice (Fig. 3c). On the other hand, the CD4 T cell numbers in mesenteric LNs (mLNs) which drain the CCL25-rich intestinal tissues³² were significantly increased in CCR9^{Tg} mice compared to WT controls (Fig. 3d), while mLN CD8 T cell numbers remained unaffected (Supplementary Fig. 7a). Such preferential accumulation of CCR9^{Tg} CD4 T cells in the mLNs was unlikely due to the increase of a particular CD4 T cell subset because the frequencies of Foxp3⁺ regulatory T cells (Tregs) and memory CD4 T cells remained unaltered between CCR9^{Tg} and control WT mice (Supplementary Fig. 7b, c). In contrast, CD4 T cell numbers in other LNs, i.e., inguinal, axillary, and submandibular LNs, which we collectively refer to as peripheral LN (pLN), did not differ between WT and CCR9^{Tg} mice (Fig. 3e). As a corollary, we found that the ratio of CD4 versus CD8 T cells was heavily skewed toward CD4 T cells in mLNs of CCR9^{Tg} mice but that it did not differ to WT mice in pLN (Fig. 3f). Considering the gut-homing function of CCR9^{13,33}, these results suggest that the forced expression of CCR9 drives the tissue distribution of CD4 T cells towards gut-associated lymphoid tissues.

Forced CCR9 expression is detrimental for the tissue trafficking of CD4⁺ SI IELs

Given the accumulation of CCR9^{Tg} CD4 T cells in gut-draining mLNs (Fig. 3d)³², we expected an increase in SI IEL CD4 T cells in CCR9^{Tg} mice. Surprisingly, this was not the case. While the overall frequency and number of SI IEL T cells did not differ between WT and CCR9^{Tg} mice (Supplementary Fig. 8a), we found that both the frequency and the number of SI IEL CD4⁺ T cells in CCR9^{Tg} mice were dramatically decreased compared to WT littermate controls (Fig. 4a and Supplementary Fig. 8b). Such a loss was specific to CD4⁺ T cells, because the number of CD8α⁺ IEL T cells remained unchanged in CCR9^{Tg} mice (Fig. 4b). Moreover, this effect was specific to CCR9, because we did not find any significant changes in the expression of other surface molecules involved in tissue migration or residency (i.e., CD69, CD103, LPAM-1 (α₄β₇), CXCR3, and CD62L) or lineage-specific transcription factors (i.e., Runx3 and ThPOK) (Supplementary Fig. 9).

SI IEL CD8 T cells comprise two distinct populations that differ in their CD8 coreceptor expression³⁴. CD8 T cells expressing the CD8αβ heterodimers correspond to conventional CD8 T cells,

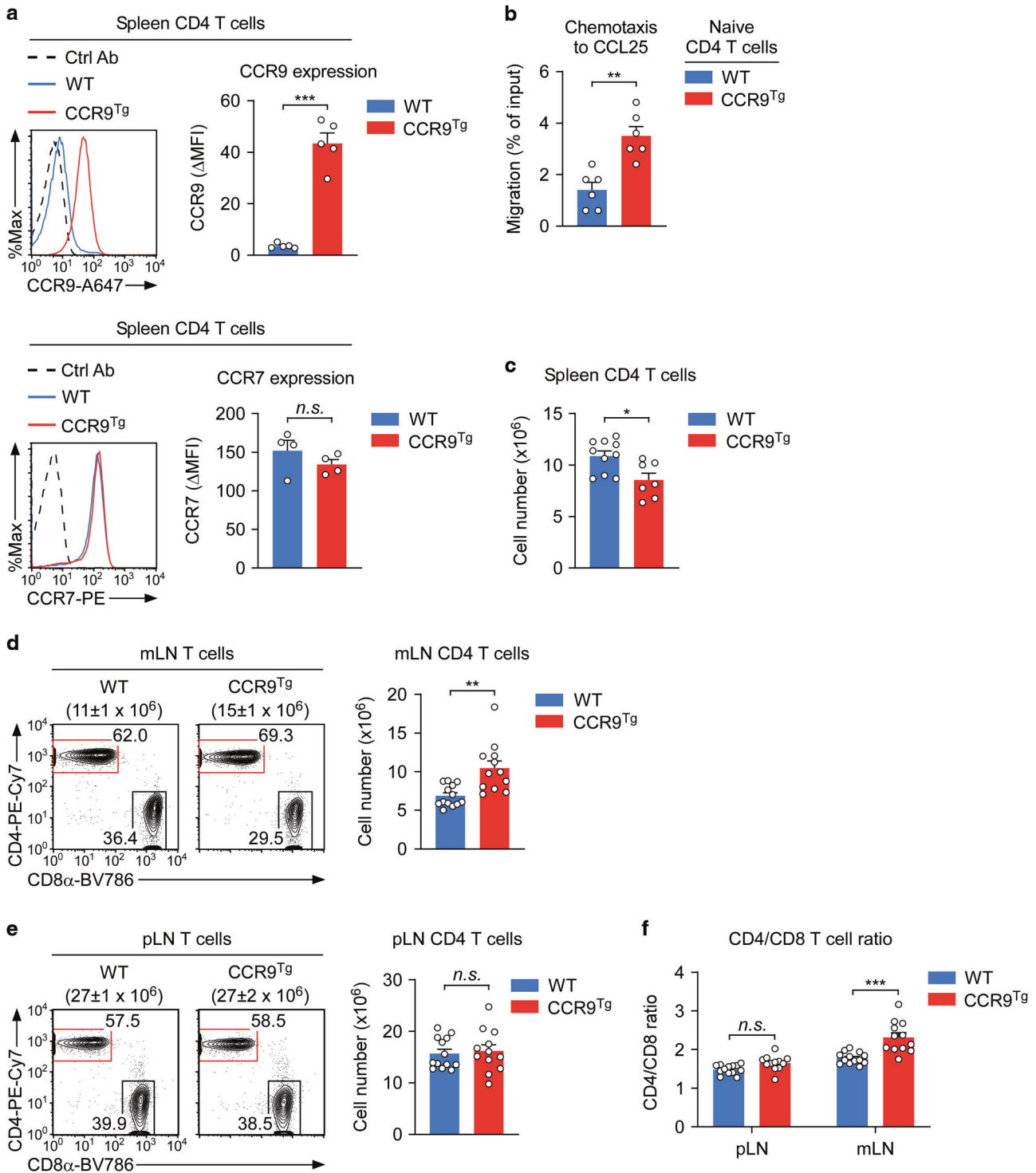
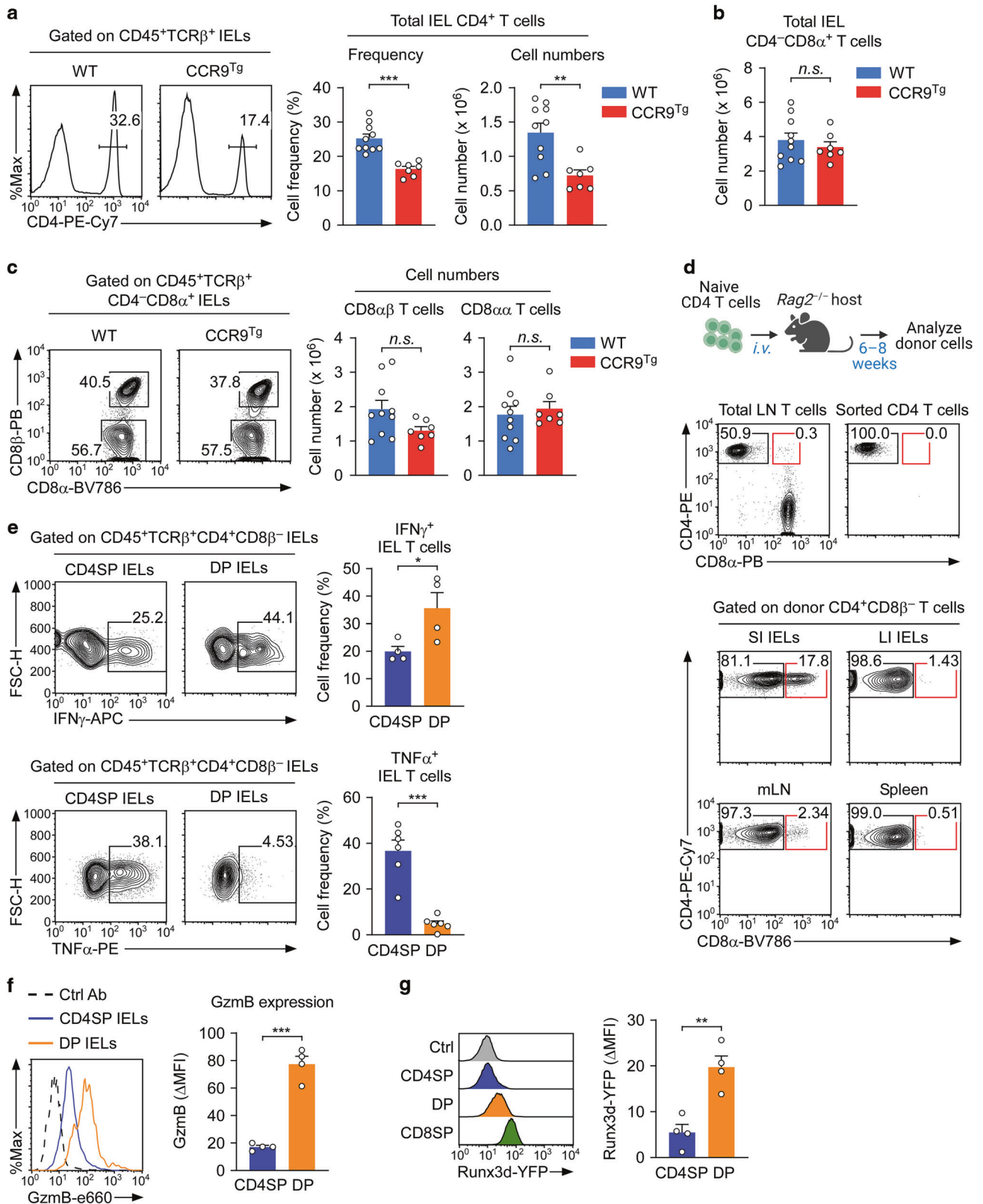


Fig. 3 Forced CCR9 expression skews peripheral tissue distribution of CD4 T cells. **a** CCR9 (top) and CCR7 (bottom) expression were assessed on CD4 spleen T cells of CCR9^{Tg} mice. Histograms are representative and graphs show summary of 5 independent experiments with a total of at least 4 WT and 4 CCR9^{Tg} mice. **b** Transwell assays for assessing chemotaxis of WT and CCR9^{Tg} naive CD4 T cells to CCL25. Data show summary of 3 independent experiments. **c** Spleen CD4 T cell numbers of WT and CCR9^{Tg} mice. Data show summary of 7 independent experiments with a total of 10 WT and 7 CCR9^{Tg} mice. **d** Frequencies and numbers of CD4 T cells in the mesenteric LNs (mLN) of WT and CCR9^{Tg} mice. Contour plots are representative, and graphs show summary of 9 independent experiments with a total of 13 WT and 12 CCR9^{Tg} mice. **e** Frequencies and numbers of CD4 T cells in the peripheral LNs (pLN) of WT and CCR9^{Tg} mice. Contour plots are representative, and graphs show summary of 9 independent experiments with a total of 13 WT and 12 CCR9^{Tg} mice. **f** CD4 versus CD8 T cell ratios in pLN and mLN of WT and CCR9^{Tg} mice. Bar graphs show summary of 9 independent experiments with a total of 13 WT and 12 CCR9^{Tg} mice. Statistical significance was determined by two-way ANOVA with Sidak's multiple comparisons test. Data are shown as mean ± SEM. **P* < 0.05, ***P* < 0.01, ****P* < 0.001, *n.s.*, not significant.



whereas CD8 T cells expressing the CD8αα homodimers are primarily found in the intestine and thought to be generated in the thymus by strong agonistic TCR signaling³⁵. We did not find any significant difference in the number of CD8αα and CD8αβ IEL T cells between CCR9^{Tg} and WT mice (Fig. 4c), affirming that CCR9

overexpression does not affect the tissue migration and residency of CD8 T cells.

Akin to CD8α⁺ IEL T cells, CD4⁺ IELs also comprise two distinct populations that differ in their CD8αα coreceptor expression, i.e., CD8αα⁺ and CD8αα-negative CD4 T cells¹⁶. CD4⁺ IEL T cells that

Fig. 4 Characterization of SI IEL T cells in CCR9^{T9} mice. **a** Frequencies and numbers of total CD4⁺ T cells among SI IEL T cells of WT and CCR9^{T9} mice. Histograms are representative, and graphs show summary of 7 independent experiments with a total of 10 WT and 7 CCR9^{T9} mice. **b** CD4⁺CD8 α ⁺ SI IEL T cell numbers of WT and CCR9^{T9} mice. Data show summary of 7 independent experiments with 10 WT and 7 CCR9^{T9} mice. **c** Frequencies and numbers of CD8 α β and CD8 $\alpha\alpha$ IEL T cells in the SI from WT and CCR9^{T9} mice. Contour plots show CD8 α versus CD8 β expression on CD8 α ⁺ IEL T cells, while the bar graphs show the summary of CD8 α β and CD8 $\alpha\alpha$ IEL T cell numbers. Data show summary of 7 independent experiments with a total of 10 WT and 7 CCR9^{T9} mice. **d** Schematic of naive CD4 T cell adoptive transfer into *Rag2*^{-/-} lymphopenic host mice (top). The purity of donor CD4 T cells was confirmed by flow cytometry (middle). Frequency of CD4⁺CD8 α ⁻ and CD4⁺CD8 $\alpha\alpha$ ⁺ DP cells among CD45.2⁺ donor CD4⁺CD8 β ⁻ T cells in the SI, large intestine (LI), mLN, and spleen of host mice was assessed after 6–8 weeks of adoptive transfer. Data are representative from 3 independent experiments. **e** Frequencies of IFN γ - (top) and TNF α -expressing (bottom) cells among CD4⁺CD8 α ⁻ (CD4SP) and CD4⁺CD8 $\alpha\alpha$ ⁺ (DP) SI IEL T cells of WT mice. Contour plots are representative, and bar graphs show summary of 3 independent experiments with at least 4 WT mice. **f** Granzyme B (GzmB) expression in CD4SP and DP SI IEL T cells of WT mice. Histograms are representative (left), and bar graphs (right) show summary of 3 independent experiments with a total of 4 WT mice. **g** *Runx3d*-YFP reporter expression was assessed on CD4SP, DP and CD4⁺CD8 $\alpha\alpha$ ⁺ (CD8SP) SI IEL T cells of *Runx3d*^{YFP/+} reporter mice. Histograms are representative (left), and bar graph (right) shows summary of 3 independent experiments with a total of 4 *Runx3d*^{YFP/+} reporter mice. Data are shown as mean \pm SEM. **P* < 0.05, ***P* < 0.01, ****P* < 0.001, *n.s.*, not significant.

do not express CD8 $\alpha\alpha$ correspond to conventional CD4 T cells (CD4SP IELs), whereas CD4 T cells that additionally express CD8 $\alpha\alpha$ appear as CD4⁺CD8 $\alpha\alpha$ ⁺. Such DP IELs are enriched in intestinal tissues¹⁹, and they mainly arise through transcriptional reprogramming of conventional CD4 T cells, specifically by inducing *Runx3* and downregulating ThPOK through T-bet-dependent processes³⁶. Adoptive transfer of naive CD4 T cells into *Rag2*-deficient lymphopenic mice can illustrate such a conversion of conventional CD4 T cells into DP T cells in vivo (Fig. 4d). Notably, such differentiation appeared to be specific to the SI epithelium because donor-origin DP T cells were found in the SI epithelium but not in the large intestine (LI) epithelium, mLN, or spleen (Fig. 4d, bottom). Whether distinct survival and tissue-specific migration also contribute to the accumulation of DP IEL T cells to the SI epithelium remains to be examined.

DP IEL T cells are considered as important immunoregulatory cells because they represent an MHCII-specific T cell population with effector function similar to CD8 cytotoxic T cells¹⁹. In this regard, DP IELs produce copious amounts of IFN γ but not TNF α (Fig. 4e) and contain high levels of the cytolytic molecule granzyme B (GzmB) (Fig. 4f). DP IEL T cells also express the transcription factor *Runx3* which is associated with cytotoxic T cell function (Fig. 4g), and they contain large amounts of the nuclear factors T-bet and Eomes which are highly expressed in effector T cells (Supplementary Fig. 10a)³⁷. On the other hand, we found that DP IELs are also capable to induce the expression of CD40L, a helper T cell-associated functional marker (Supplementary Fig. 10b)³⁸. Thus, DP IELs occupy a special niche in T cell immunity as they display both CD8 and CD4 T lineage effector phenotypes in the context of MHCII-associated antigens.

Characterization of CD4⁺CD8 $\alpha\alpha$ ⁺ DP IEL T cells in CCR9^{T9} mice

To examine whether CCR9 would affect the differentiation of DP T cells in the SI epithelium, we next extracted SI IELs from WT and CCR9^{T9} mice and enumerated DP T cells among the IELs. While DP IEL T cells comprise around 4% of all IEL T cells in WT mice (Fig. 5a), strikingly, both the frequency and number of these cells were dramatically reduced in CCR9^{T9} mice (Fig. 5a). DP IELs are derived from conventional CD4 IEL T cells, and the frequency of DP IELs among CD4⁺CD8 β ⁻ IEL T cells was substantially reduced (Fig. 5b), suggesting that CCR9 impedes the differentiation of CD4 into DP T cells. In agreement, the ratio of DP versus CD4SP IELs was dramatically diminished in CCR9^{T9} mice (Fig. 5b). Altogether, these results revealed that the forced expression of CCR9 impairs the tissue trafficking and the phenotypic conversion of CD4 IEL T cells.

The differentiation of CD4 into DP SI IELs is associated with the loss of *Foxp3*⁺ expressing cells which correspond to regulatory T cells (Tregs)³⁹. Indeed, *Foxp3*-GFP reporter expression revealed a paucity of *Foxp3*⁺ cells in DP IELs (Fig. 5c). Thus, we next wished to examine whether CCR9 overexpression would result in the

accumulation of *Foxp3*⁺ Treg cells among CD4 IEL T cells. However, this turned out to be not the case. We did not find a significant difference in *Foxp3*⁺ IEL Treg cell frequencies as demonstrated using *Foxp3*-GFP reporter mice (Fig. 5c), indicating that the effect of CCR9 overexpression is specific to DP IEL T cells without affecting *Foxp3*⁺ Treg cells.

Because CCR9 gain-of-function (CCR9^{T9}) resulted in the loss of DP IEL T cells, we next aimed to examine if CCR9 loss-of-function would conversely promote the differentiation of CD4 IEL T cells into DP cells. To this end, we obtained CCR9-deficient (CCR9^{KO}) mice and assessed SI IELs of these mice. Notably, the lack of CCR9 induced a substantial increase in both the frequency and number of DP IEL T cells, while CD4SP IEL T cell numbers were unaffected (Fig. 5d and Supplementary Fig. 11a), revealing a previously unappreciated role for CCR9 in the generation of DP T cells in the SI epithelium. Again, such an effect was specific to the loss of CCR9 expression, because there were no significant changes in the expression of surface molecules involved in tissue migration or residency (i.e., CD69, CD103, LPAM-1 ($\alpha_4\beta_7$), CXCR3, and CD62L) or lineage-specific transcription factor (*Runx3* and ThPOK) (Supplementary Fig. 11b).

Forced CCR9 expression impairs the differentiation of CD4⁺CD8 $\alpha\alpha$ ⁺ DP IEL T cells

To understand how CCR9 would impact the differentiation of CD4 IEL T cells, we considered that the conversion of CD4 into CD4⁺CD8 $\alpha\alpha$ ⁺ DP IEL T cells requires engagement with MHCII that is expressed on SI epithelial cells (ECs)⁴⁰. Notably, MHCII expression is unevenly distributed along the SI so that the proximal SI, which comprises the duodenum and the jejunum, expresses low amounts of MHCII while the distal SI, corresponding to the ileum, expresses large amounts of MHCII⁴¹. In agreement with such distinct MHCII expression, we found that DP IELs were mostly absent in the duodenum/jejunum compared with the ileum where we found DP IELs to be enriched (Fig. 6a). Thus, the conversion of CD4 to DP IELs is a spatially constrained event that is inefficient in the duodenum/jejunum and that requires access to distal SI tissues⁴¹.

To examine how the forced expression of CCR9 would limit the access of CD4 T cells to ECs in the ileum, we next assessed chemokine expression in the intestine. To this end, we analyzed a published RNA-seq dataset of ECs from the duodenum, jejunum, and ileum of the SI for the abundance of different chemokines⁴¹. Consistent with previous reports⁴², we found that CCL25 was highly expressed in intestinal ECs (Fig. 6b). We further noticed that CCL25 was mostly produced by ECs in the duodenum and jejunum, but only at low levels in the ileum (Fig. 6c), which we further confirmed by assessing CCL25 mRNA expression in these sites (Fig. 6d). These results revealed a gradient of CCL25 abundance whereby the proximal SI would attract CCR9-expressing T cells while the distal SI would fail to do so. Such a

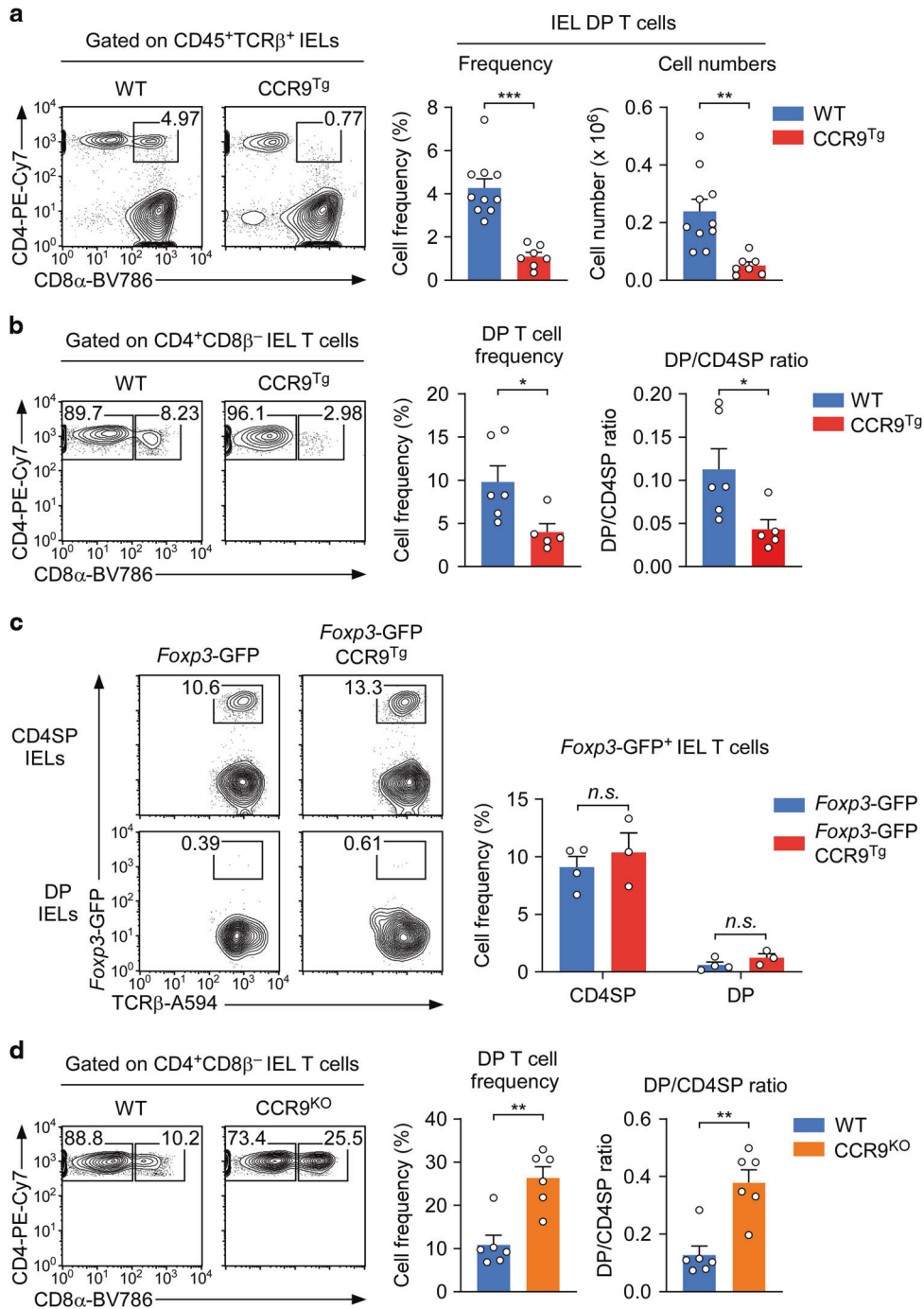
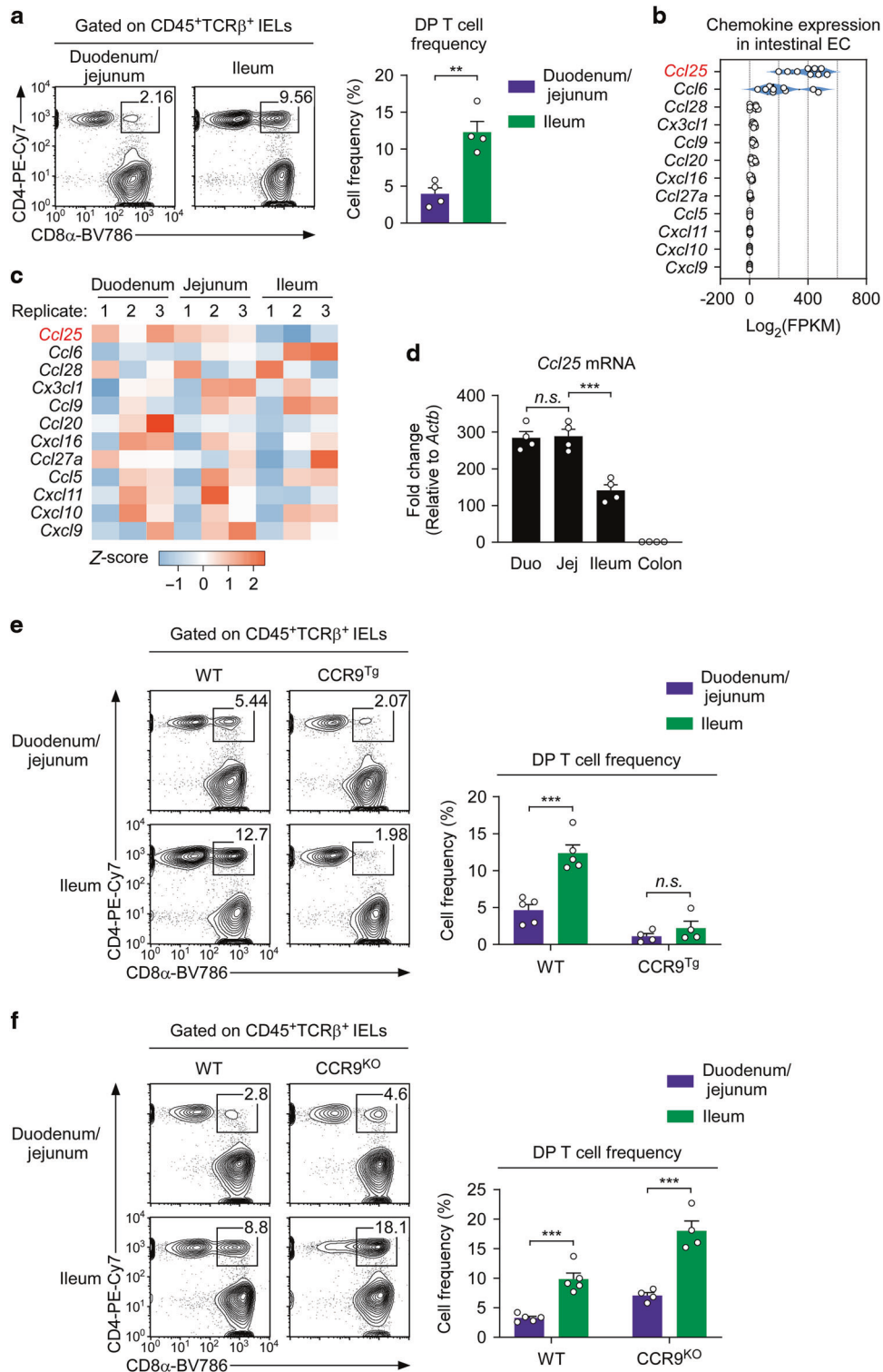


Fig. 5 Forced expression of CCR9 is detrimental for the differentiation of DP IEL T cells. **a** Frequencies and numbers of DP IEL T cells in the SI epithelium of WT and CCR9^{Tg} mice. Contour plots are representative, and bar graphs show summary of 7 independent experiments with a total of 10 WT and 7 CCR9^{Tg} mice. **b** DP IEL frequencies among CD4⁺CD8β⁻ T cells of WT and CCR9^{Tg} mice. Contour plots are representative, and bar graphs show summary of 5 independent experiments with a total of 6 WT and 5 CCR9^{Tg} mice. **c** Frequencies of *Foxp3*-GFP⁺ Tregs in CD4SP and DP SI IEL T cells of *Foxp3*-GFP reporter and *Foxp3*-GFP-CCR9^{Tg} mice. Contour plots are representative, and bar graph shows summary of 3 independent experiments with a total of 4 *Foxp3*-GFP and 3 *Foxp3*-GFP-CCR9^{Tg} mice. Statistical significance was determined by two-way ANOVA with Sidak's multiple comparisons test. **d** DP IEL frequencies among CD4⁺CD8β⁻ T cells of WT and CCR9^{KO} mice. Contour plots are representative (left), and bar graphs (right) show summary of 4 independent experiments with a total of 6 WT and 6 CCR9^{KO} mice. Data are shown as mean ± SEM. **P* < 0.05, ***P* < 0.01, ****P* < 0.001, n.s., not significant.

chemokine gradient was specific to CCL25, because CCL6, another chemokine that is highly expressed in intestinal tissues (Fig. 6b), was mostly produced in the distal SI (Fig. 6c).

Consequently, we hypothesized that the forced expression of CCR9 would attract CD4 IEL T cells to the proximal SI, resulting in the enrichment of CD4 IEL T cells in the duodenum/jejunum. If

such was the case, we hypothesized that CD4 T cell migration into the ileum would be relatively impaired in CCR9^{Tg} mice. In the SI of WT mice, the ileum harbors 2.3-fold higher frequencies of CD4 T cells than the duodenum/jejunum (Supplementary Fig. 12a). In CCR9^{Tg} mice, however, we found that the frequency of CD4 IEL T cells in the ileum was significantly blunted and that it increased



only 1.5-fold compared to the duodenum/jejunum (Supplementary Fig. 12a). In agreement, CD4 IEL T cell numbers in the ileum of CCR9^{Tg} mice were also dramatically decreased (Supplementary Fig. 12b). Consequently, the generation of DP IELs, which mostly occurs in the distal part of the SI⁴¹, was markedly impaired in CCR9^{Tg} mice (Fig. 6e and Supplementary Fig. 12b). In contrast, CCR9-deficiency promoted the generation of DP IELs, so that CCR9^{KO} mice showed a dramatic increase in CD4⁺CD8α⁺ IELs in the ileum compared to WT controls (Fig. 6f). Therefore, these

genetic models of CCR9 gain- and loss-of functions reveal CCR9 expression as a regulatory pathway of DP IEL differentiation.

Finally, to demonstrate that CCR9-mediated effects are T cell intrinsic, we set up adoptive transfer experiments where CCR9^{Tg} and congenic WT naive CD4 T cells were mixed at 1:1 ratio and injected into *Rag2*-deficient lymphopenic host mice (Supplementary Fig. 13a). Prior to injection, we confirmed that the FACS-sorted donor CD4 T cell populations were completely void of CD4⁺CD8α⁺ DP cells and that they have been mixed at correct

Fig. 6 Tissue-specific mapping of CCR9-mediated differentiation of DP IEL T cells. **a** Frequencies of DP IEL T cells in WT mice were assessed in the proximal (duodenum/jejunum) and distal (ileum) parts of the SI epithelium. Contour plots are representative (left), and bar graph (right) shows summary of 2 independent experiments with a total of 4 WT mice. Statistical significance was determined by paired two-tailed Student's *t*-test. **b** Chemokine expression in SI epithelial cells (ECs) was assessed using public RNA-seq datasets and visualized as violin plots for individual chemokines. **c** Heatmap of chemokine expression in different parts of SI ECs. Public RNA-seq data of SI ECs from the duodenum, jejunum, and ileum were analyzed, and the site-specific chemokine expression was assembled as heatmap. **d** RT-qPCR analyses of CCL25 mRNA expression normalized to β -actin mRNA in the indicated gut tissues of WT mice. Data show summary of 2 independent experiments. Statistical significance was assessed by one-way ANOVA with Tukey's multiple comparisons test. **e** Frequencies of DP IELs in different parts of the SI epithelium of WT and CCR9^{Tg} mice. Contour plots are representative (left), and bar graph (right) shows summary of 4 independent experiments with a total of 5 WT and 4 CCR9^{Tg} mice. Statistical significance was determined by two-way ANOVA with Sidak's multiple comparisons test. **f** Frequencies of DP IELs in the indicated parts of the SI epithelium of WT and CCR9^{KO} mice. Contour plots are representative (left), and bar graph (right) shows summary of 4 independent experiments with a total of 5 WT and 4 CCR9^{KO} mice. Statistical significance was determined by two-way ANOVA with Sidak's multiple comparisons test. Data are shown as mean \pm SEM. ***P* < 0.01, ****P* < 0.001, *n.s.*, not significant.

ratios (Supplementary Fig. 13b). Six to eight weeks after transfer, donor T cells were harvested from the mLN and the SI epithelium and assessed for the repopulation of the tissues. While we found a clear but statistically insignificant increase in CCR9^{Tg} CD4 T cell accumulation in the mLN (Supplementary Fig. 13c, left), we noticed a marked reduction in the CCR9^{Tg}-origin CD4 T cells in the SI epithelium (Supplementary Fig. 13c, right). Moreover, we found that WT donor CD4 T cells efficiently differentiated into CD4⁺CD8 α ⁺ IELs but that CCR9^{Tg}-origin CD4 T cells were severely blunted in their differentiation, resulting in dramatically reduced frequencies and numbers of DP IELs (Supplementary Fig. 13d). Altogether, the results indicated that the acquired CCL25 responsiveness in CCR9^{Tg} CD4 T cells impedes the generation of DP IELs, presumably due to alterations in tissue trafficking and distribution of CD4 T cells in SI epithelial tissues (Supplementary Fig. 14).

DISCUSSION

Here, we aimed to address why CCR9 is downregulated on most CD4 but not on CD8 T cells, and whether such a lack of CCR9 would be critical for the proper development, differentiation, and tissue distribution of CD4 T cells. To this end, we generated CCR9 transgenic mice that ectopically express functional CCR9 on CD4 T cells, and we found that CCR9 did not interfere with the thymic development of CD4 T cells but altered their tissue tropism and differentiation in the periphery. In particular, the forced expression of CCR9 resulted in the quantitative loss of CD4 IELs, accompanied by impaired differentiation of CD4⁺CD8 α ⁺ DP IELs, thus unveiling a detrimental effect of CCR9. Collectively, these results suggested that CCR9 downregulation is a mechanism that ensures effective gut tropism and intestinal differentiation of CD4 T cells.

CCR9 expression is dynamically regulated during T cell development in the thymus, starting in hematopoietic progenitor cells that express large amounts of CCR9 but is lost after seeding the thymus. Therefore, Early Thymic Progenitors (ETPs) that are found among DN1 stage thymocytes cease to express CCR9¹⁰. The differentiation of ETPs into DN3 stage cells, which is associated with successful β -selection⁴³, results in the re-expression of CCR9, induced by the transcription factors HEB and E2A¹⁰. CCR9 then remains highly expressed through thymocyte development and persists on mature CD8 T cells. The lineage commitment into CD4 T cells, however, triggers the rapid downregulation of CCR9, resulting in a dichotomy of CCR9 expression between CD4 and CD8 T cells. Consequently, CD4SP thymocytes and mature CD4 T cells, but not CD8 lineage T cells, lack CCR9. Mechanistically, it has not been clear whether CCR9 expression is actively suppressed in CD4 T cells or whether CD4 T cells fail to upregulate the expression of CCR9. Accordingly, we considered two possibilities to explain the contrasting CCR9 expression between CD4 and CD8 T cells. First, we hypothesized that CCR9 is exclusively expressed on CD8 T cells because CD8 T cells would

contain factors that drive the expression of CCR9. We considered Runx3 as a likely candidate molecule. Runx3 is specifically expressed on CD8 but not on CD4 lineage T cells and was previously found to promote the expression of multiple factors associated with CD8 T cell function, such as granzyme B, perforin, and CD103⁴⁴. To assess whether this would be the case, we examined CCR9 expression on CD4 T cells that were forced to express Runx3²⁴, but found that Runx3 was insufficient to induce CCR9 expression. Moreover, we found that CD8 T cells from Runx3d-deficient mice still expressed CCR9. These results suggested that Runx3 is neither necessary nor sufficient for CCR9 expression, effectively excluding Runx3 as a regulator of CCR9 expression. As a second possibility, we hypothesized that CD4 T cells may specifically express a suppressor of CCR9 expression, resulting in the downregulation of CCR9. In this regard, we noted that the transcriptional repressor ThPOK is exclusively found in CD4 lineage cells and absent in immature thymocytes and mature CD8 T cells⁴⁵, mirroring the CCR9 expression in T cell development. Thus, we predicted that ThPOK-deficient CD4 T cells would fail to suppress CCR9 expression, while CD8 T cells that are forced to express ThPOK would downregulate CCR9 expression. Unfortunately, an experimental system to test this hypothesis is not available. ThPOK is critical for CD4 lineage specification so that ThPOK-deficiency prevents the generation of CD4 T cells²⁶. Therefore, it is difficult to know whether ThPOK-deficient CD4 T cells would upregulate CCR9 expression because such CD4 T cells cannot be generated²⁶. Along these lines, it is impractical to examine whether the forced expression of ThPOK would suppress CCR9 expression in CD8 T cells because the ectopic expression of ThPOK blocks the generation of CD8 T cells and redirects lineage choice into CD4 T cells^{25,26}. Nonetheless, in support of a CCR9 suppressor function of ThPOK, we found that *i*NKT cells, which is another major thymocyte population that express ThPOK, had downregulated CCR9 expression to the same extent as conventional CD4 T cells. Overexpression of ThPOK also further suppressed CCR9 expression on CD4 IEL T cells, which we found to contain markedly reduced amounts of ThPOK compared to spleen CD4 T cells. These results agree with a potential role of ThPOK in CCR9 downregulation, but this remains to be directly demonstrated. Interestingly, by scanning the *Ccr9* gene for potential ThPOK binding sites, we identified a putative ThPOK consensus binding site ~12 kb upstream of the *Ccr9* coding region, which we aim to test in the future for a functional role in regulating the expression of CCR9.

Considering the abundance of CCL25 in the thymus, it remained puzzling to us that the forced expression of CCR9 minimally affected the development and maturation of CD4 T cells. While CCR9^{Tg} mice have been previously generated and described⁴⁶, the CCR9^{Tg} thymocytes in our study differed from the CCR9^{Tg} cells in the original report by the Love group where CCR9 overexpression severely impaired thymopoiesis and interfered with the intrathymic localization of CD25⁺ DN2/3 thymocytes⁴⁶. More specifically,

the total thymocyte numbers of our CCR9^{Tg} mice did not substantially differ from those of littermate controls, and the frequency of CD25⁺ DP thymocytes also did not significantly increase (data not shown), which differs to the CCR9^{Tg} mice in the Uehara study⁴⁶. As a potential explanation, we postulate that the amount of transgenic CCR9 differs between the CCR9^{Tg} lines, causing different phenotypes depending on the abundance of CCR9. In fact, the Uehara study already showed that the thymic phenotype of CCR9^{Tg} mice varied between different founders, depending on the amount of transgenic CCR9 expression⁴⁶. Thus, potential phenotypic differences between the different lines of CCR9^{Tg} mice, including those of our study, can be attributed to the distinct amounts of CCR9 expression in these mice.

While we did not notice any major effects of CCR9 overexpression in thymic CD4 T cells, it was interesting to find that the tissue distribution of peripheral CCR9^{Tg} CD4 T cells was disarranged. Because CCR9 overexpression increased the sensitivity to CCL25, we expected that CCR9^{Tg} CD4 T cells would be altered in their tissue tropism. In this regard, we observed a decrease in circulating CCR9^{Tg} CD4 T cells, as documented by the reduced numbers of spleen CD4 T cells. However, in contrast to our expectation, CCR9^{Tg} CD4 T cells did not preferentially migrate to and accumulate in the thymus and the intestine, the two most prominent sites of CCL25 expression^{31,47}. Instead, we found that CCR9^{Tg} CD4 T cells accumulated in mLNs, which was associated with a loss of CCR9^{Tg} CD4 T cells among SI IELs. Why CCR9 overexpression would induce the accumulation of CD4 T cells in mLN is currently unclear to us. Potentially, CCL25, which is abundantly produced by SI epithelial cells³¹, could be diffused and become highly concentrated in the draining mLNs, thus attracting CCR9^{Tg} CD4 T cells. However, this possibility remains to be experimentally tested.

A prominent outcome of CCR9-deficiency is a defect in CD8 T cell recruitment to the small intestinal mucosa^{7,8}. Because CCR9 is a gut tropic chemokine receptor, such results are expected. In contrast, the CD4 T cell compartment remains undisturbed in CCR9-deficient mice⁷, agreeing with the notion that CD4 T cells normally do not express CCR9 and therefore CCR9-deficiency should not alter their tissue distribution. Thus, we initially postulated that forced expression of CCR9 on CD4 T cells would promote their gut tropism. Surprisingly, CCR9 overexpression did not promote but rather impaired the accumulation of CD4 T cells among SI IELs, which was contrary to our expectations. Here, we wish to point out that, unlike other peripheral CD4 T cells, SI IEL CD4 T cells do express discernible amounts of CCR9⁴⁸. Such CCR9 expression is an acquired phenotype imposed by the gut environment, mostly through the vitamin A metabolite, RA⁴⁸. Because peripheral CD4 T cells in CCR9^{Tg} mice are forced to express functional CCR9 prior to their entry to the gut mucosa, we consider it likely CCR9⁺ CD4 T cells can be recruited to CCL25-rich tissue sites other than the SI epithelium, diminishing the migration of CCR9^{Tg} CD4 T cells to the gut epithelium. As a corollary, we would expect that CD4 T cells in CCR9^{Tg} mice that are also deficient for CCL25 could be spared from such constraints and freely migrate into SI epithelial tissues. However, this remains to be tested. Alternatively, the diminished accumulation of CCR9^{Tg} CD4 T cells in the SI epithelium could have been the result of their increased expulsion into the intestinal lumen or greater egress from gut tissues. These possibilities have been considered but not experimentally addressed in our current study, thus, imposing some limitations on the interpretation of our results.

A key finding of the forced expression of CCR9 on CD4 T cells was its unexpected and deleterious effect on CD4⁺CD8 α ⁺ DP IEL T cells. DP T cells in the SI epithelium are proposed to exert immunoregulatory function by expressing pro-inflammatory cytokines and displaying cytolytic function^{18,19,49}. Despite their importance, however, the molecular mechanisms controlling the differentiation of CD4⁺CD8 α ⁺ SI IEL T cells have remained

incompletely understood. A role for the gut microbiota⁵⁰ or MHCI1 and PD-L1 expression has been previously reported⁴¹, but thus far chemokine receptors have not been implicated in this process. Our finding that CCR9 gain-of-function in CD4 T cells impairs, while CCR9 loss-of-function promotes the differentiation of DP IELs now highlights a previously unappreciated role for a chemokine receptor in the regulation of intraepithelial T cell differentiation.

Altogether, our data demonstrated that premature and ectopic expression of CCR9 is detrimental for the normal tissue distribution of CD4 T cells. Moreover, we identified ThPOK as a potential driver of CCR9 suppression in T cells, which—if confirmed—would supply the molecular basis of the CD4 lineage specific loss of CCR9 during T cell differentiation. Consequently, CCR9 downregulation is hardwired into CD4 T cell differentiation, and our results reveal that such a process is necessary to optimize CD4 T cell trafficking and effector T cell differentiation in the gut.

MATERIALS AND METHODS

Mice

C57BL/6Ncr1 (C57BL/6) mice were obtained from the Charles River Laboratories. *Rag2*^{-/-} (*Rag*^{KO}) mice and *Ccr9*^{-/-} (*CCR9*^{KO}) mice⁷ were purchased from The Jackson Laboratory. CCR9-transgenic (CCR9^{Tg}) mice were generated in this study by ligating mouse *Ccr9* cDNA under the control of the human *CD2* promoter/enhancer. *Runx3*^{Tg} mice were previously described²⁴. *Runx3d*^{YFP/+} and *Runx3d*^{YFP/YFP} (*Runx3d*^{KO}) mice were previously reported²³ and acquired through The Jackson Laboratory. ThPOK-transgenic mice (ThPOK^{Tg}) were previously described⁵¹, and generously provided by Dr. Remy Bosselut. *CD40*^{-/-} mice were previously described⁵², and kindly provided by Dr. Richard J. Hodes. ThPOK-GFP reporter mice were kindly provided by Dr. Ichiro Taniuchi²⁷. *Foxp3*-GFP knock-in reporter mice were a gift from Dr. Vijay K. Kuchroo⁵³. *Foxp3*-GFP-CCR9^{Tg} mice were generated by crossing CCR9^{Tg} mice with *Foxp3*-GFP knock-in reporter mice. Animal experiments were performed using 8- to 12-weeks old mice. Sex- and age- matched C57BL/6 or littermates were used as wild-type (WT) controls. All animal experiments were reviewed and approved by the NCI Animal Care and Use Committee. NCI-Frederick is accredited by AAALAC International and follows the Public Health Service Policy for the Care and Use of Laboratory Animals. Animal care was provided in accordance with the procedures outlined in the "Guide for Care and Use of Laboratory Animals (National Research Council; 1996; National Academy Press; Washington, D.C.).

Flow cytometry

Single-cell suspensions were stained with fluorescence-conjugated antibodies as previously described for surface staining and intracellular staining⁵⁴. The following antibodies were used: CCR9 (CW-1.2), TCR β (H57-597), CD45 (30-F11), CCR7 (4B12), CD24 (M1/69), CD45.1 (A20), CXCR3 (CXCR3-173), CD103 (2E7), LPAM-1 (DATK32), CD40L (MR1), TNF α (MP6-XT22), IFN γ (XMG1.2), mouse IgG2a κ Isotype (MOPC-173) and MHCI (AF6-88.5) from BioLegend (San Diego, CA); CD8 β (eBioH35-17.2), CD44 (IM7), CD45.2 (104), GzmB (NGZB), T-bet (eBio4B10 (4B10)), Eomes (Dan11mag), mouse IgG1 kappa Isotype (P3.6.2.8.1) and *Foxp3* (FJK-16) from ThermoFisher eBioscience; CD8 α (53-6-7), CD62L (MEL-14), CD69 (H1.2F3), CD25 (PC61.5), *Runx3* (R3-5G4), ThPOK (T43-94), mouse IgG1 κ Isotype (MOPC-31C) and CD16/32 (2.4G2) from BD Biosciences (San Jose, CA); CD4 (GK1.5), and Ghost Dye™ Violet 510 from Tonbo Biosciences. CD1d tetramers loaded with PBS-57 were obtained from the NIH tetramer facility (Emory University, Atlanta, GA). *Foxp3*, *Runx3*, ThPOK, T-bet and Eomes intracellular staining was performed using *Foxp3* intracellular staining buffer set (eBioscience). GzmB, TNF α and IFN γ intracellular staining was performed using IC fixation kit (eBioscience), according to the manufacturer's instructions. For TNF α and IFN γ expression assessment, cells were incubated for 4 h in the presence of PMA (50 ng/mL; Sigma-Aldrich) and ionomycin (1 μ M; Sigma-Aldrich) and with 1 μ g/mL brefeldin A (Invitrogen) for the final 3 h before staining. For assessing CD40L expression, *CD40*^{-/-} mice were used to exclude the possibility that CD40L is internalized by CD40³⁸, and IELs were stimulated with PMA (50 ng/mL) and ionomycin (1 μ M) for 2 h before surface staining. Flow cytometry samples were analyzed using LSRll or LSRFortessa (BD Bioscience). Flow cytometry data were analyzed with FlowJo v10.6.2 software.

Lymphocyte isolation

Single-cell suspensions were generated from peripheral lymph nodes (pLN, including inguinal, brachial, axillary, and submandibular, but not mLN), mLNs, spleen, and thymus by passing the tissues through 100 μ m nylon filters (Merck Millipore). IELs from SI or large intestine (LI) were isolated as previously described⁵⁵. In brief, SI and LI were harvested and washed in HBSS containing 2% FCS, followed by shaking in 25 mL of solution A media (10% FCS, 0.0154 g DL-dithiothreitol, and 1% 0.5 M EDTA in HBSS) at 240 rpm for 45 min. IELs from the SI were recovered from the supernatant of solution A media, and epithelial cells (ECs) were removed from the cell suspension by negative selection using anti-EpCAM antibody (clone G8.8, eBiosciences), followed by magnetic separation with BioMag beads (Qiagen). IELs from LI were recovered using 40/80% Percoll gradients (GE Healthcare) with centrifugation at 2000 rpm for 25 min at room temperature. Cells were placed on ice until further analysis by flow cytometry. Where indicated, the SI was separated into two parts by cutting the junction between the jejunum and ileum as described previously before washing⁵⁶.

Naive CD4 T cell isolation

Naive CD4 T cells were isolated using MojoSort™ Mouse CD4 Naive T Cell Isolation Kits (Biolegend), according to the manufacturer's instructions. In brief, total LN and spleen cells were pooled, washed with Mojosort buffer, and filtered through 70 μ m Falcon filters. Cells were resuspended in MojoSort™ buffer at 100×10^6 cells/mL, followed by incubation with the provided antibody cocktail and Streptavidin Nanobeads for 15 min, successively. Naive CD4 T cells were collected after magnetic separation and kept in 10% FCS-supplemented RPMI-1640 medium on ice until further use.

Chemotaxis assay

Chemotaxis assays were performed as previously described⁹. Briefly, naive CD4 T cells from WT or CCR9^{T9} mice were starved for 1 h in RPMI-1640 medium supplemented with 0.5% BSA (0.5% BSA-medium) before loading into transwell inserts. One hundred μ L of cell suspension containing 5×10^5 cells was added to the upper chamber of the 5 μ m pore inserts (Corning) in wells containing 600 μ L of 0.5% BSA-medium with or without 300 nM CCL25 (R&D Systems). After 4 h of incubation at 37 °C, the cells in the bottom wells were collected and counted for live cells using Trypan blue counterstaining. Cells that migrated under this condition without CCL25 were considered as spontaneously migrated cells. Duplicate wells were used for each condition.

Adoptive transfer of naive CD4 T cells

Naive CD4 T cells (CD44^{lo}) were sorted from LN cells of C57BL/6 mice, CD45.1⁺ congenic C57BL/6 mice or CCR9^{T9} mice (CD45.2⁺). FACS-sorted cells were checked for their purity by flow cytometry, and washed in PBS before adoptive transfer. For assessing DP IEL differentiation in different organs, each 5×10^6 naive CD4 T cells from C57BL/6 mice were intravenously injected into the tail vein of *Rag2*^{-/-} host mice. For competitive adoptive transfer experiments, sorted naive CD4 T cells from CD45.1⁺ congenic mice or CD45.2⁺ CCR9^{T9} mice were mixed at 1:1 ratio, and a total of 1×10^7 cells were intravenously injected into the tail vein of *Rag2*^{-/-} host mice. Because the naive CD4 T cells were not sorted based on CD45RB expression, the adoptive transfer into lymphopenic host mice did not result in colitis induction. After 6–8 weeks of transfer, donor cells were recovered from host mice and assessed by flow cytometry.

Real-time quantitative PCR analysis

Total RNA was isolated from different tissues (e.g., the duodenum, jejunum, and ileum of the SI, and the colon) of C57BL/6 mice using the RNeasy Plus Mini Kit (Qiagen) and then reverse-transcribed into cDNA with the QuantiTect Reverse Transcription kit (Qiagen) according to manufacturer's instructions. Real-time quantitative PCR (RT-qPCR) was then performed with the QuantiTect SYBR Green detection system (Qiagen) on the QuantiStudio 6 RT-PCR instrument (Life Technologies). The primer sequences were as follows: *Actb* (forward: 5'-GAGAGGGAAATCGTGCCTGA-3'; reverse: 5'-ACATCTGCTGGAAGGTGG-3'), *Ccl25* (forward: 5'-TTACCAGCACAGGATCAAATGG-3'; reverse: 5'-CGGAAGTAGAATCTCACAGCAC-3').

Public RNA sequencing data analysis

The database used in this study is publicly available from The European Bioinformatics Institute (EMBL-EBI) under accession numbers E-MTAB-9744

and E-MTAB9756⁴¹. The processed data with log₂ transformed fragments per kilobase of transcript per million mapped reads value (log₂ FPKM) was used to analyze chemokine expression on intestinal ECs. Heatmap of chemokine expression in all samples was generated in R language using the "heatmap3" package.

Statistical analysis

Data are shown as mean \pm SEM. Statistical significance was determined by unpaired two-tailed Student's *t*-test, except where specifically indicated in the figure legends. *P* values of less than 0.05 were considered significant. **P* < 0.05, ***P* < 0.01, ****P* < 0.001, *n.s.*, not significant. All statistical analysis was performed using GraphPad Prism 8 software (GraphPad software).

REFERENCES

- Calderon, L. & Boehm, T. Three chemokine receptors cooperatively regulate homing of hematopoietic progenitors to the embryonic mouse thymus. *Proc. Natl Acad. Sci. USA* **108**, 7517–7522 (2011).
- Plotkin, J., Prockop, S. E., Lepique, A. & Petrie, H. T. Critical role for CXCR4 signaling in progenitor localization and T cell differentiation in the postnatal thymus. *J. Immunol.* **171**, 4521–4527 (2003).
- Kadokia, T. et al. E-protein-regulated expression of CXCR4 adheres preselection thymocytes to the thymic cortex. *J. Exp. Med.* **216**, 1749–1761 (2019).
- Kurobe, H. et al. CCR7-dependent cortex-to-medulla migration of positively selected thymocytes is essential for establishing central tolerance. *Immunity* **24**, 165–177 (2006).
- Misslitz, A. et al. Thymic T cell development and progenitor localization depend on CCR7. *J. Exp. Med.* **200**, 481–491 (2004).
- Choi, Y. I. et al. PlexinD1 glycoprotein controls migration of positively selected thymocytes into the medulla. *Immunity* **29**, 888–898 (2008).
- Uehara, S., Grinberg, A., Farber, J. M. & Love, P. E. A role for CCR9 in T lymphocyte development and migration. *J. Immunol.* **168**, 2811–2819 (2002).
- Wurzel, M. A. et al. Mice lacking the CCR9 CC-chemokine receptor show a mild impairment of early T- and B-cell development and a reduction in T-cell receptor $\gamma\delta^+$ gut intraepithelial lymphocytes. *Blood* **98**, 2626–2632 (2001).
- Wurzel, M. A., Malissen, B. & Campbell, J. J. Complex regulation of CCR9 at multiple discrete stages of T cell development. *Eur. J. Immunol.* **36**, 73–81 (2006).
- Krishnamoorthy, V. et al. Repression of *Ccr9* transcription in mouse T lymphocyte progenitors by the Notch signaling pathway. *J. Immunol.* **194**, 3191–3200 (2015).
- Ohoka, Y., Yokota, A., Takeuchi, H., Maeda, N. & Iwata, M. Retinoic acid-induced CCR9 expression requires transient TCR stimulation and cooperativity between NFATc2 and the retinoic acid receptor/retinoid X receptor complex. *J. Immunol.* **186**, 733–744 (2011).
- Cassani, B. et al. Gut-tropic T cells that express integrin $\alpha 4\beta 7$ and CCR9 are required for induction of oral immune tolerance in mice. *Gastroenterology* **141**, 2109–2118 (2011).
- Svensson, M. et al. CCL25 mediates the localization of recently activated CD8 $\alpha\beta^+$ lymphocytes to the small-intestinal mucosa. *J. Clin. Investig.* **110**, 1113–1121 (2002).
- Xu, Y. et al. In Vivo Generation of Gut-Homing Regulatory T Cells for the Suppression of Colitis. *J. Immunol.* **202**, 3447–3457 (2019).
- Guy-Grand, D. et al. Two gut intraepithelial CD8⁺ lymphocyte populations with different T cell receptors: a role for the gut epithelium in T cell differentiation. *J. Exp. Med.* **173**, 471–481 (1991).
- Cheroutre, H., Lambomez, F. & Mucida, D. The light and dark sides of intestinal intraepithelial lymphocytes. *Nat. Rev. Immunol.* **11**, 445–456 (2011).
- Olivares-Villagomez, D. & Kaer, Van L. Intestinal Intraepithelial Lymphocytes: Sentinels of the Mucosal Barrier. *Trends Immunol.* **39**, 264–275 (2018).
- Van Kaer, L. & Olivares-Villagomez, D. Development, Homeostasis, and Functions of Intestinal Intraepithelial Lymphocytes. *J. Immunol.* **200**, 2235–2244 (2018).
- Zhou, C., Qiu, Y. & Yang, H. CD4CD8 $\alpha\alpha$ IELs: They Have Something to Say. *Front. Immunol.* **10**, 2269 (2019).
- Mucida, D. et al. Transcriptional reprogramming of mature CD4(+) helper T cells generates distinct MHC class II-restricted cytotoxic T lymphocytes. *Nat. Immunol.* **14**, 281–289 (2013).
- Xing, Y., Wang, X., Jameson, S. C. & Hogquist, K. A. Late stages of T cell maturation in the thymus involve NF- κ B and tonic type I interferon signaling. *Nat. Immunol.* **17**, 565–573 (2016).
- Singer, A., Adoro, S. & Park, J. H. Lineage fate and intense debate: myths, models and mechanisms of CD4- versus CD8-lineage choice. *Nat. Rev. Immunol.* **8**, 788–801 (2008).
- Egawa, T. & Littman, D. R. ThPOK acts late in specification of the helper T cell lineage and suppresses Runx-mediated commitment to the cytotoxic T cell lineage. *Nat. Immunol.* **9**, 1131–1139 (2008).
- Keller, H. R. et al. The molecular basis and cellular effects of distinct CD103 expression on CD4 and CD8 T cells. *Cell Mol. Life Sci.* **78**, 5789–5805 (2021).

25. Luckey, M. A. et al. The transcription factor ThPOK suppresses Runx3 and imposes CD4(+) lineage fate by inducing the SOCS suppressors of cytokine signaling. *Nat. Immunol.* **15**, 638–645 (2014).
26. He, X., Park, K. & Kappes, D. J. The role of ThPOK in control of CD4/CD8 lineage commitment. *Annu. Rev. Immunol.* **28**, 295–320 (2010).
27. Muroi, S. et al. Cascading suppression of transcriptional silencers by ThPOK seals helper T cell fate. *Nat. Immunol.* **9**, 1113–1121 (2008).
28. Engel, I. et al. Co-receptor choice by Va14i NKT cells is driven by Th-POK expression rather than avoidance of CD8-mediated negative selection. *J. Exp. Med.* **207**, 1015–1029 (2010).
29. Wang, L. et al. The sequential activity of Gata3 and Thpok is required for the differentiation of CD1d-restricted CD4⁺ NKT cells. *Eur. J. Immunol.* **40**, 2385–2390 (2010).
30. Sun, G. et al. The zinc finger protein cKrox directs CD4 lineage differentiation during intrathymic T cell positive selection. *Nat. Immunol.* **6**, 373–381 (2005).
31. Wurbel, M.-A. et al. The chemokine TECK is expressed by thymic and intestinal epithelial cells and attracts double- and single-positive thymocytes expressing the TECK receptor CCR9. *Eur. J. Immunol.* **30**, 262–271 (2000).
32. Houston, S. A. et al. The lymph nodes draining the small intestine and colon are anatomically separate and immunologically distinct. *Mucosal Immunol.* **9**, 468–478 (2016).
33. Pabst, O. et al. Chemokine receptor CCR9 contributes to the localization of plasma cells to the small intestine. *J. Exp. Med.* **199**, 411–416 (2004).
34. Imhof, B. A., Dunon, D., Courtois, D., Luhtala, M. & Vainio, O. Intestinal CD8 $\alpha\alpha$ and CD8 $\alpha\beta$ intraepithelial lymphocytes are thymus derived and exhibit subtle differences in TCR β repertoires. *J. Immunol.* **165**, 6716–6722 (2000).
35. Leishman, A. J. et al. Precursors of Functional MHC Class I- or Class II-Restricted CD8 $\alpha\alpha$ ⁺ T Cells Are Positively Selected in the Thymus by Agonist Self-Peptides. *Immunity* **16**, 355–364 (2002).
36. Reis, B. S., Hoytema van Konijnenburg, D. P., Grivennikov, S. I. & Mucida, D. Transcription factor T-bet regulates intraepithelial lymphocyte functional maturation. *Immunity* **41**, 244–256 (2014).
37. Intlekofer, A. M. et al. Effector and memory CD8⁺ T cell fate coupled by T-bet and eomesodermin. *Nat. Immunol.* **6**, 1236–1244 (2005).
38. Lesley, R., Kelly, L. M., Xu, Y. & Cyster, J. G. Naive CD4 T cells constitutively express CD40L and augment autoreactive B cell survival. *Proc. Natl Acad. Sci. USA* **103**, 10717–10722 (2006).
39. Sujino, T. et al. Tissue adaptation of regulatory and intraepithelial CD4(+) T cells controls gut inflammation. *Science* **352**, 1581–1586 (2016).
40. Bilate, A. M. et al. T Cell Receptor Is Required for Differentiation, but Not Maintenance, of Intestinal CD4(+) Intraepithelial Lymphocytes. *Immunity* **53**, 1001–1014.e1020 (2020).
41. Moon, S. et al. Niche-specific MHC II and PD-L1 regulate CD4⁺CD8 $\alpha\alpha$ ⁺ intraepithelial lymphocyte differentiation. *J. Exp. Med.* **218**, e20201665 (2021).
42. Zabel, B. A. et al. Human G protein-coupled receptor GPR-9-6/CC chemokine receptor 9 is selectively expressed on intestinal homing T lymphocytes, mucosal lymphocytes, and thymocytes and is required for thymus-expressed chemokine-mediated chemotaxis. *J. Exp. Med.* **190**, 1241–1256 (1999).
43. Rothenberg, E. V., Moore, J. E. & Yui, M. A. Launching the T-cell-lineage developmental programme. *Nat. Rev. Immunol.* **8**, 9–21 (2008).
44. Shan, Q. et al. The transcription factor Runx3 guards cytotoxic CD8(+) effector T cells against deviation towards follicular helper T cell lineage. *Nat. Immunol.* **18**, 931–939 (2017).
45. He, X. et al. CD4-CD8 lineage commitment is regulated by a silencer element at the ThPOK transcription-factor locus. *Immunity* **28**, 346–358 (2008).
46. Uehara, S. et al. Premature expression of chemokine receptor CCR9 impairs T cell development. *J. Immunol.* **176**, 75–84 (2006).
47. Kunkel, E. J. et al. Lymphocyte CC chemokine receptor 9 and epithelial thymus-expressed chemokine (TECK) expression distinguish the small intestinal immune compartment: Epithelial expression of tissue-specific chemokines as an organizing principle in regional immunity. *J. Exp. Med.* **192**, 761–768 (2000).
48. Iwata, M. et al. Retinoic acid imprints gut-homing specificity on T cells. *Immunity* **21**, 527–538 (2004).
49. Das, G. et al. An important regulatory role for CD4⁺CD8 $\alpha\alpha$ T cells in the intestinal epithelial layer in the prevention of inflammatory bowel disease. *Proc. Natl Acad. Sci. USA* **100**, 5324–5329 (2003).
50. Cervantes-Barragan, L. et al. Lactobacillus reuteri induces gut intraepithelial CD4(+)CD8 $\alpha\alpha$ (+) T cells. *Science* **357**, 806–810 (2017).
51. Wang, L. et al. The zinc finger transcription factor Zbtb7b represses CD8-lineage gene expression in peripheral CD4⁺ T cells. *Immunity* **29**, 876–887 (2008).
52. Kawabe, T. et al. The immune responses in CD40-deficient mice: impaired immunoglobulin class switching and germinal center formation. *Immunity* **1**, 167–178 (1994).
53. Bettelli, E. et al. Reciprocal developmental pathways for the generation of pathogenic effector TH17 and regulatory T cells. *Nature* **441**, 235–238 (2006).
54. Park, J. Y. et al. CD24⁺ Cell Depletion Permits Effective Enrichment of Thymic iNKT Cells While Preserving Their Subset Composition. *Immune Netw.* **19**, e14 (2019).
55. Prakhar, P., Gonzalez, V. & Park, J. H. High-yield enrichment of mouse small intestine intraepithelial lymphocytes by immunomagnetic depletion of EpCAM⁺ cells. *STAR Protoc.* **3**, 101207 (2022).
56. Stephens, R. H., Tanianis-Hughes, J., Higgs, N. B., Humphrey, M. & Warhurst, G. Region-dependent modulation of intestinal permeability by drug efflux transporters: in vitro studies in mdr1a(-/-) mouse intestine. *J. Pharm. Exp. Ther.* **303**, 1095–1101 (2002).

ACKNOWLEDGEMENTS

We thank Drs. Paul Love (NICHD) and Yousuke Takahama (NCI) for critical review of this manuscript. This study has been supported by the Intramural Research Program of the US National Institutes of Health, National Cancer Institute, Center for Cancer Research. This project has been also funded in part with Federal funds from the National Cancer Institute, National Institutes of Health, under Contract No. HHSN2612015000031. The content of this publication does not necessarily reflect the views or policies of the Department of Health and Human Services, nor does mention of trade names, commercial products, or organizations imply endorsement by the U.S. Government.

AUTHOR CONTRIBUTIONS

C.L. designed and performed experiments, analyzed data, and contributed to the writing of the manuscript. H.K., P.P., S.L., A.C., D.L., M.L., and P.A. performed experiments, analyzed data, and commented on the manuscript. R.G. provided expertise and reviewed, commented on the manuscript. J.P. conceived the project, analyzed the data, and wrote the manuscript.

COMPETING INTERESTS

The authors declare no competing interests.

ADDITIONAL INFORMATION

Supplementary information The online version contains supplementary material available at <https://doi.org/10.1038/s41385-022-00540-9>.

Correspondence and requests for materials should be addressed to Jung-Hyun Park.

Reprints and permission information is available at <http://www.nature.com/reprints>

Publisher's note Springer Nature remains neutral with regard to jurisdictional claims in published maps and institutional affiliations.